# Adaptive Sensor Tasking Strategies for Tracking Non-Cooperative Cislunar Space Objects

**Jeremy Correa, John Ware**
*Katalyst Space Technologies*
**Maruthi R. Akella, Brandon A. Jones**
*The University of Texas at Austin*

## ABSTRACT

Growing interest and activity in cislunar space have highlighted the need for enhanced space domain awareness (SDA) and space situational awareness (SSA) capabilities. Non-cooperative space objects can execute unexpected maneuvers or reveal concealed capabilities, making conventional tracking and sensor management strategies less effective. This paper outlines a framework designed to provide automated sensor tasking and facilitate the maintenance of tracking data for multiple target objects in cislunar space, using existing sensor platforms and architectures. To establish this framework, research efforts were focused on: (1) developing locally optimal sensor tasking strategies for space-based panchromatic (VIS) sensors, (2) developing multi-target observation association techniques to detect non-cooperative tracking events, and (3) designing a scalable and modular software architecture with open architecture concepts to enable flexibility, adaptability, and robustness in simulating cislunar space operations.

## 1. INTRODUCTION

Recent interest and activity in cislunar space have highlighted the need to extend space domain awareness (SDA) capabilities to ensure safe operations for existing and planned missions in geostationary orbit and beyond. Effective SDA in the cislunar regime requires the ability to search for, detect, and predict the trajectories of cislunar space objects, including those previously unknown. This challenge is further complicated by non-cooperative space objects that may execute unanticipated maneuvers or reveal concealed capabilities, making conventional tracking and sensor management strategies less effective. Due to these compounding challenges and increased mission complexity in the cislunar regime, the imperative for system architectures that support automation of tactical decision making and sensor tasking becomes increasingly clear.

In response to these challenges, the ICON (Interoperable Cislunar Observation Network) architecture was developed to optimize sensor usage for detecting, tracking, and tasking in cislunar space. ICON utilizes existing sensors to perform local searches, facilitate object tracking, and generate tasking recommendations for other assets. Figure 1 illustrates a mission concept for ICON and the key capabilities required to accomplish localized search and cooperative tracking via decentralized tasking to accomplish strategic mission objectives in cislunar space.

This paper focuses on our approach to the object tracking and sensor tasking portions of this architecture. Techniques for optimized decentralized search and tasking are explored, specifically for an architecture with multiple sensors tracking a single object of interest. A scenario is created to simulate accurate cislunar dynamics, realistic sensor capabilities, and probable trajectories for objects of interest. Simplifications and assumptions are explained throughout, in an effort to focus the simulation on local search and tasking methods. Although there are numerous scenarios in the cislunar regime whereby non-cooperative space objects can impede tracking efforts, this paper focuses on a reference scenario that involves tracking a space object in transit between the Earth and Moon with the capability to execute impulsive maneuvers and deploy unknown objects.

The approach used to construct sensor tasking schedules leverages a semi-Markov Decision Process (SMDP) as the fundamental mathematical framework. Situations are considered where target states are well-known, direct observations are feasible, and localized searches of targets when covariance growth exceeds manageable thresholds. Over a finite planning horizon, we are able to generate locally optimal sensor tasking strategies that aim to minimize tracking uncertainty and improve the quality of state estimates of non-cooperative space objects. The approach enables cooperative tracking of multiple target objects through selective information sharing and aggregation of track data across multiple sensing platforms.

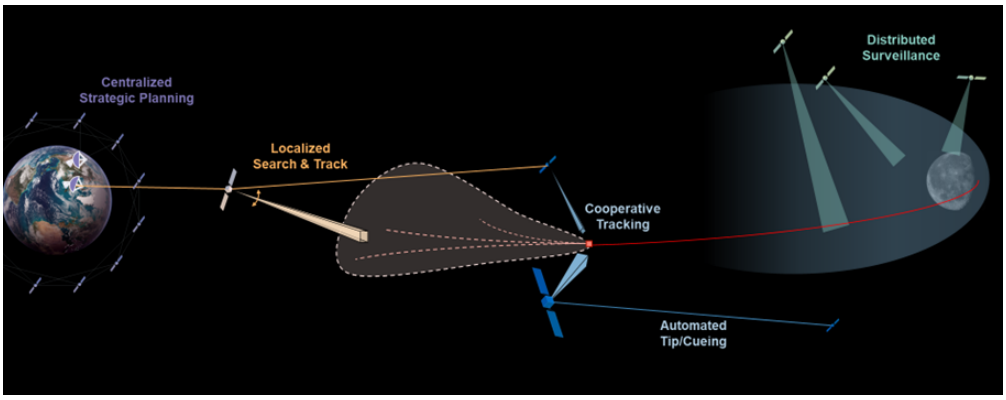


Fig. 1: Distributed, Interoperable Cislunar Observation Network

This paper first provides a background on the problem of maintaining custody of non-cooperative objects in cislunar space and introduces the associated challenges in Section 2. Section 3 focuses on the localized search and tracking framework, detailing how search regions are transformed into sensor measurement space. In Section 4, we introduce the adaptive sensor tasking approach, designed to optimize multi-sensor scheduling in dynamic tracking environments. Section 5 presents the results of the simulation, demonstrating the framework's effectiveness in tracking a maneuvering target in the Earth-Moon system. Finally, Section 6 summarizes the findings and explores potential directions for future work.

## 2. PROBLEM FORMULATION

Chaotic dynamics in cislunar space and the large volume of XGEO space create significant challenges for maintaining custody of space objects. Small maneuvers can result in large trajectory changes, and present opportunities for objects of interest to affect the near-Earth regime. Here we consider the problem of constructing tasking schedules across multiple space-based sensing platforms to observe and estimate the state of a non-cooperative resident space object (RSO) in cislunar space. Several simplifications and assumptions are made to enable an initial simulation.

The motion of both the target and the observer (sensor) is modeled using the circular restricted three-body problem (CRTBP). The state of the system, consisting of position $\mathbf{r}$ and velocity $\mathbf{v}$, evolves according to the following dynamics:

$$\dot{\mathbf{r}} = \mathbf{v}, \quad \dot{\mathbf{v}} = \mathbf{g} + \eta_g \tag{1}$$

where $\mathbf{g}$ is the gravitational acceleration based on the CRTBP model, and $\eta_g$ represents noise or perturbations affecting the system. Gravitational acceleration $\mathbf{g}$ is expressed as:

$$\mathbf{g} = -2\mathbf{n}\times\mathbf{r} - \mathbf{n}\times(\mathbf{n}\times\mathbf{r}) - \frac{1-\mu}{|\mathbf{r}_1|^3}\mathbf{r}_1 - \frac{\mu}{|\mathbf{r}_2|^3}\mathbf{r}_2 \tag{2}$$

Here, $\mathbf{r}_1$ and $\mathbf{r}_2$ represent the position vectors of the spacecraft relative to the Earth and Moon, respectively, and $\mu = \frac{m_{Moon}}{m_{Earth}+m_{Moon}}$ is the mass ratio between the Earth and Moon. The term $\mathbf{n} = \begin{bmatrix}0 & 0 & 1\end{bmatrix}^T$ accounts for the rotational frame of reference. To model impulsive maneuvers of the target, we include an additional control input $\mathbf{u}_{\Delta v}$ that updates the velocity at discrete times. The velocity immediately after an impulsive maneuver is updated as:

$$\mathbf{v}^+ = \mathbf{v}^- + \mathbf{u}_{\Delta v} \tag{3}$$

where $\mathbf{v}^-$ and $\mathbf{v}^+$ represent the velocity before and after the maneuver, respectively, and $\mathbf{u}_{\Delta v}$ represents the impulsive change in velocity due to the maneuver.

This paper assumes each of the participating sensors are passive optical sensors. We assume an angles-only (az, el) measurement model, where the azimuth, elevation, and apparent range to the target are given by [2],

$$\hat{z}_0 = \hat{h}_0(\hat{m}) = \begin{bmatrix}\hat{h}_\alpha(\hat{m})\\ \hat{h}_\varepsilon(\hat{m})\\ \hat{h}_\rho(\hat{m})\end{bmatrix} = \begin{bmatrix}\hat{\alpha}\\ \hat{e}\\ \hat{\rho}\end{bmatrix} = \begin{bmatrix}\tan^{-1}\left(\frac{i_y}{i_x}\right)+\eta_\alpha\\ \sin^{-1}(i_z)+\eta_e\\ \left|\hat{\mathbf{r}}_{\text{target}}-\hat{\mathbf{r}}_{\text{obs}}\right|+\eta_\rho\end{bmatrix} \tag{4}$$

The vector $\hat{\mathbf{r}}_{\text{obs}}$ represents the position of the observer, and $\hat{\mathbf{r}}_{\text{target}}$ represents the position of the target in the Earth-Moon synodic reference frame. Noise is added to each measurement ($\eta_\alpha$, $\eta_e$, and $\eta_\rho$). The estimated relative line-of-sight between the observer and target is defined by $\hat{\mathbf{i}}_\rho = \begin{bmatrix} i_x & i_y & i_z \end{bmatrix}^T$.

The photometric signatures of target objects are simplified by approximating that they are diffuse Lambertian spheres reflecting light in the visible spectrum. The apparent visual magnitude is given by,

$$m_{v,app}(\alpha_g, \Omega, \varphi) = m_{v,sun} - 2.5\log_{10}\left(\alpha_g \cdot \frac{A}{r^2} \cdot f(\varphi)\right) \tag{5}$$

where $m_{v,sun} = -26.74$ is the apparent visual magnitude of the sun, $\alpha_g$ is the approximate spectrally-independent geometric albedo, $\Omega = \frac{A}{r^2}$ is the solid angle subtended by the cross-section of the target at the sensor, and $f(\varphi)$ is the phase angle dependent scattering function. For the scattering function, this analysis will utilize the function for a diffuse reflecting sphere, derived by Vallerie [3],

$$f(\varphi) = \frac{2}{3\pi}\left[\sin(\varphi) + (\pi - \phi)\cos(\varphi)\right] \tag{6}$$

In the proposed scenario, a heterogenous sensing architecture has the strategic goal of tracking an unknown space object transiting the Earth-Moon system. Each sensor is assumed to be able to contribute to the collective strategic goal in a limited capacity due to resource allocation constraints and tasking priority. Because of this, we will be exploring the viability of generating automated sensor tasking across the sensor architecture to optimally search for and track the unknown space object.

The exemplar target trajectory was computed via conjugated gradient descent. The trajectory is composed of 3 maneuvers to transit from LEO to 10km perilune, from 10km perilune to the GEO belt, and a final maneuver to enter retro-GEO. The exemplar target trajectory, shown in Figure 2, was computed via conjugated gradient descent, consisting of three maneuvers from low Earth orbit (LEO) to retro-GEO, with a lunar assist.

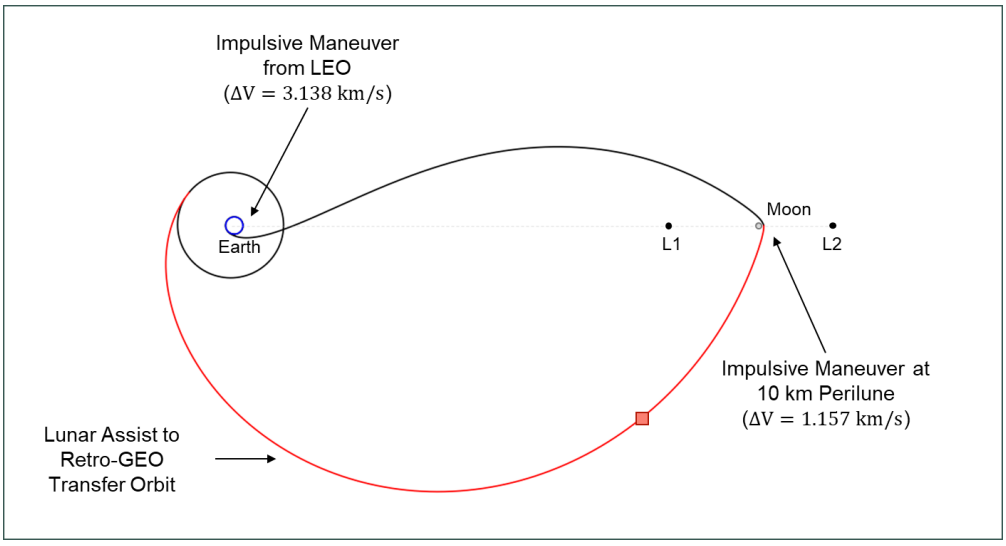


Fig. 2: Visualization of LEO to retro-GEO trajectory with a lunar assist

## 3. LOCALIZED SEARCH AND TRACKING

### 3.1 Localized Search Strategies and Sensor Pointing Schema

Missions with space situational awareness (SSA) objectives will require the ability to detect and track objects within their operational domain. Within the context of the cislunar domain, efficient sensor resource allocation can quickly become a complex challenge when operations teams are required to balance strategic mission objects and their tactical execution in an uncertain environment. Some primary reasons for these challenges include imperfect sensing conditions, limited sensor resources, and operational demands that may temporarily divert sensors away from tracking tasks. During periods of limited availability, state uncertainty and error can grow significantly, especially when compounded by imperfect sensing conditions or sensors being tasked with other activities. Additionally, the presence of non-cooperative behaviors, such as unexpected maneuvers by space objects, can further contribute to growing state uncertainty, making it more difficult to maintain an accurate estimate of the target's position.

This paper proposes an interoperable search strategy designed to efficiently reduce uncertainty in dynamic operational environments. Once an object is detected, a tracklet is created from a series of observations. Propagating this tracklet enables the creation of a localized search area based on a subset of potential and likely trajectories. This search area is broken into a grid, and the primary sensor is tasked to perform a raster scan of the area based on sensor parameters such as field of view, availability, and occlusions. Figure 3 shows a depiction of this concept. For the purposes of this effort, the scan pattern does not take into account probability distributions for search regions, though this is an area for future work towards operational systems.

**Construction of Search Volumes** A sensor is prompted to execute a localized search by receiving a tracking tip message from an external source. In operations, this would be a message from another satellite or ground station, but in an effort to limit complexity, we assume that this information is transmitted on a limited basis and do not model constraints associated with establishing inter-satellite or ground links. The tracking tip message is mathematically defined as:

$$\mathcal{M}_{\text{track}} = (t_k, \mathbf{x}_k, P_k) \tag{7}$$

where $t_k$ is the time of the last track update, $\mathbf{x}_k$ is the estimated state vector of the target, and $P_k$ is the estimated target covariance at the specified time.

Candidate search tasks are constructed by first propagating the estimated target state and uncertainty to the expected search window. The transformed state is then projected into the sensor's reference frame. Next, the projected region is mapped directly into the sensor's measurement space (azimuth-elevation angles). The search volume is discretized into a grid of azimuth-elevation cells, with spacing determined by the sensor's angular resolution. The region is constrained within the covariance ellipse and the sensor's field-of-view (FOV) half-angle, represented by:

$$(\omega - \mathbf{x}_k^o)^\intercal P_k^{-1} (\omega - \mathbf{x}_k^o) \leq 3\sigma^2 \quad \textit{and} \quad |\omega - \mathbf{x}_k^o| \leq \frac{\theta_{FOV}}{2} \tag{8}$$

where $\omega$ is a candidate grid point in the azimuth-elevation space, $\mathbf{x}_k^o$ is the estimated target state, and $P_k$ is the estimated target covariance, both expressed in azimuth-elevation coordinates. The covariance ellipse is defined such that it encompasses points within a 3-sigma confidence interval, which represents the region where the target is most likely to be found, based on the estimated state and uncertainty. Figure 3 shows an idealized visual depiction of a target uncertainty volume discretized into collection opportunities.

**Search Region Transformation** The sensor is modeled at the center of gravity (CG) of its host spacecraft and is assumed to be able to steer in both pitch and yaw. The transformation from the Earth-Moon synodic reference frame to the sensor's local frame involves translating all objects in the environment (including uncertainty volumes) inversely from the sensor's position to the origin and rotating the frame such that the sensor is positioned at the origin and facing the -z axis (denoted as the w-axis here).

The position transformation is given by $\mathbf{R}_{EM}^{uvw} = \begin{bmatrix} \hat{\mathbf{u}} & \hat{\mathbf{v}} & \hat{\mathbf{w}} \end{bmatrix}^\intercal$ where $\hat{\mathbf{w}} = \frac{\mathbf{r}_o - \mathbf{r}_t}{\|\mathbf{r}_o - \mathbf{r}_t\|}$ , $\hat{\mathbf{u}} = \hat{\mathbf{w}} \times \mathbf{n}$ is the cross product of the normal vector $\mathbf{n}$ and $\hat{\mathbf{w}}$, and $\hat{\mathbf{v}} = \hat{\mathbf{w}} \times \mathbf{u}$.

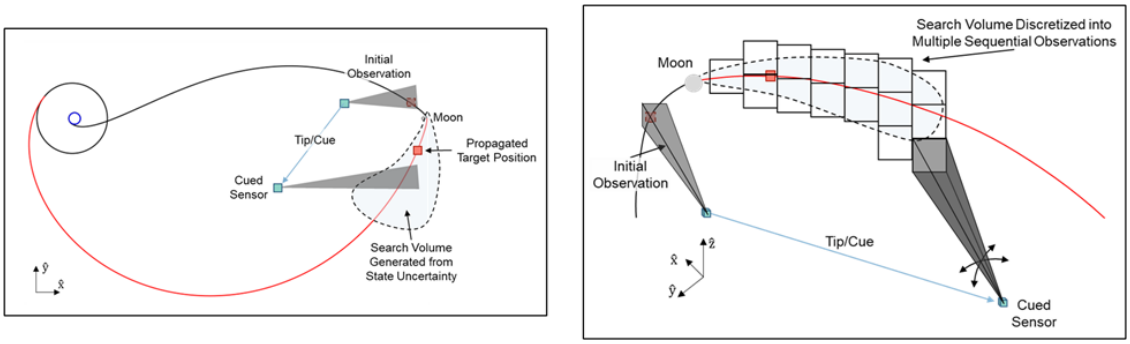


Fig. 3: Visualization of Localized Search

The transformation into azimuth-elevation coordinates (Line-of-Sight, LOS) for measurements is given by:

$$los = \begin{bmatrix} \theta \\ \phi \\ \rho \end{bmatrix} = \begin{bmatrix} \tan^{-1}(u/-w) \\ \tan^{-1}\left(v/\sqrt{u^2+w^2}\right) \\ \sqrt{u^2+v^2+w^2} \end{bmatrix} \tag{9}$$

where $u$, $v$, and $w$ are the coordinates in the sensor's local frame.

The corresponding measurement covariance transformation is given by:

$$\mathbf{P}_{\text{azel}} = \mathbf{J}\mathbf{P}_{\text{uvw}}\mathbf{J}^{\mathsf{T}}, \tag{10}$$

where $\mathbf{J}$ is the Jacobian of the azimuth-elevation transformation with respect to the sensor's local coordinates $(u, v, w)$.

**Search Task Generation** The process of converting an uncertainty search region into sensor tasks involves generating a sequence of pointing configurations and collection times based on the sensor's capabilities. These tasks are designed to provide a leak-proof way to search an uncertainty region and find a target. These cells are then sequenced using a raster scan pattern. Although raster scans provide a straightforward means to structure the search, more efficient strategies, such as prioritizing the center of the uncertainty region where the target is more likely to be, could improve detection. For now, raster scans are employed as a simplification.

To represent a search task, we define a tuple:

$$\mathcal{T}_{i,\text{search}} = (t_{\text{start}}, t_{\text{end}}, T_c, P_c)$$

where $t_{\text{start}}$ and $t_{\text{end}}$ define the time window for the search task, $T_c$ is the set of collection times, and $P_c$ is the set of pointing configurations.

## 4. MULTI-SENSOR ADAPTIVE TASKING FOR TRACKING NON-COOPERATIVE RSOS

As an object of interest transits the Earth-Moon corridor, it can quickly exit the area of custody generated by a primary sensor. Once an object is identified by a primary sensor and a tracklet is created, we calculate availability and applicability of other sensors in the region to determine which sensors could potentially gain or maintain custody of the object. These additional sensors are autonomously tasked to point in a given direction and/or perform a local search. Availability and applicability of additional sensors is determined by a custom reward function. Inputs to the function include sensor position, imaging capabilities, physical occlusions, and tasking freedom.

Transferring and maintaining custody across multiple sensors further reduces position and velocity uncertainty of an object over time. It is assumed that tasking recommendations can be shared across platforms via mission operations connections on the ground, though it is not assumed these sensors must be identical or operated by the same organization. This scenario enables new sensor configurations and capabilities to be imported and tasked appropriately for these search objectives. For the purposes of this experiment, it is assumed each sensor has limited availability for search tasks, with individual observations spaced out in time by several hours. This value is configurable to accommodate partial tasking for multipurpose missions, and in future work this will be dependent on individual sensor capabilities, availability, and occlusions.

### 4.1 MDP Formulation

In this paper, the multi-sensor scheduling problem is posed as a semi-Markov Decision Process (sMDP). Formulating the sensor scheduling problem as an MDP has been done for a variety of mission domains and applications, [1]. With respect to this proposed implementation, we consider a system consisting of $N$ agents, where the $i$-th agent can perform a set of feasible actions that could have a positive, negative, or neutral affect on the system's state. Actions are chosen based on their predicted consequences and are ultimately promoted for scheduling and converted to sensor tasking. We define the MDP as

$$\mathcal{M} = (\mathcal{A}, \mathcal{S}, \mathcal{T}, \mathcal{R}) \tag{11}$$

where $\mathcal{A} = \{a_0, a_1, \ldots, a_M\}$ is the action space and $a_j$ is a candidate action; $\mathcal{S} = \{s_0, s_1, \ldots, s_N\}$ is the state space; $\mathcal{T}(s_{i,k+1} \mid s_{i,k}, a_i)$ is the state transition function; and $\mathcal{R}(s_{i,k}, a_j)$ is the reward function, which evaluates the effectiveness of taking action $a_j$ in state $s_{i,k}$ for the i-th agent.

**Action Space** The action space $A$ represents all feasible actions that can be performed by participating agents given their current state. The primary actions considered are:

- **Localized Search**: An agent performs a search within a specified uncertainty volume by slewing between line-of-sight (LOS) vectors, settling, and performing collections. This action is feasible when the agent is not actively tracking a target, and when the estimated target uncertainty projected into the sensor reference frame exceeds the size of the sensor's field of view. Given the target's estimated state $\mathbf{x}_k$ and associated covariance matrix $P_k$ at time $t_k$, the search area is constrained to points within the covariance region. Candidate search tasks are enumerated for all agents and are defined mathematically as a tuple:

$$\mathcal{T}_{i,\text{search}} = (t_{\text{start}}, t_{\text{end}}, T_c, P_c) \tag{12}$$

  where $t_{\text{start}}$ and $t_{\text{end}}$ define the time window for the search task, $T_c$ is the set of collection times, and $P_c$ is the set of pointing configurations.

- **Tracking**: Once a target is detected, the agent transitions to a state where tracking tasks become feasible. In this state, the agent can be scheduled to execute recurring observations over a specified window of opportunity. The set of observation windows is denoted by $\mathcal{W}$, where each window is associated with a set of specific observation times defined by:

$$t_{\text{meas}}(i, j) = t_0 + i \cdot \Delta t_{\text{window}} + j \cdot t_{\text{integration}}, \tag{13}$$

  where $\Delta t_{\text{window}} = n_{\text{consecutive\_obs}} \cdot t_{\text{integration}} + t_{\text{gap}}$ represents the total duration of an observation window, $i \in \{0, 1, \ldots, n_{\text{windows}} - 1\}$ indexes the observation windows, and $j \in \{0, 1, \ldots, n_{\text{consecutive\_obs}} - 1\}$ indexes the observations within each window. The complete observation schedule is given by the set of times: $\{t_{\text{meas}}(i, j) \mid t_{\text{meas}}(i, j) \leq t_f\}$ within each window in $\mathcal{W}$. The tracking tasks are defined mathematically as a tuple:

$$\mathcal{T}_{i,\text{track}} = (t_{\text{start}}, t_{\text{end}}, \mathcal{W}, P_c) \tag{14}$$

where $t_{\text{start}}$ and $t_{\text{end}}$ define the time window for the tracking task, $\mathcal{W}$ is the set of observation windows, and $P_c$ is the set of pointing configurations.

**State Space** The state space $\mathcal{S}$ encompasses all possible satellite states at a given time. Each satellite state $s_i \in \mathcal{S}$ includes the satellite's current position, velocity, and attitude, tasking availability, and a track catalog that contains the latest estimated state and covariance of targets.

**Reward Function** The reward function $R(s,a)$ for a given state $s$ and action $a$ assigns a value to each state transition based on its effectiveness in achieving a mission objective. This is currently defined as a weighted summation of select performance metrics.

$$R(s,a) = \sum_{i=1}^{n} w_i \cdot m_i(s,a), \tag{15}$$

where $w_i$ are the weights assigned to each metric $m_i(s,a)$, and $n$ is the total number of metrics considered.

**Action Termination** Search actions terminate update target detection or after searching the uncertainty volume is finished. Tracking actions terminates when the observation window $[t_0, t_f]$ concludes or when external data necessitates a policy change. For instance, if the target maneuvers unexpectedly or a higher-priority task arises, the tracking action may be paused or adjusted.

### 4.2 Event-Driven Policy Adjustment

In the event of a significant state change, satellite behavioral policies are automatically adjusted in an effort to promote high-quality decision making. In the context of the localized search problem, a satellite policy $\pi$ is a mapping from the state space $\mathcal{S}$ to the action space $\mathcal{A}$, defining the behavior or decision making tendencies under different state conditions. Given a current satellite state $s_k \in \mathcal{S}$, the policy $\pi(s_k)$ specified the subset of actions $a_k \in \mathcal{A}$ that the satellite should consider scheduling.

**Maximum Search Time Threshold** This is a event-driven mechanism designed to limit the time a satellite spends on a localized search operation when attempting to reacquire a target within a predefined uncertainty region. Formally, let $t_{\text{search}}$ denote the cumulative search time for a given target, and $T_{\max}$ represent the maximum allowable search time threshold. The policy adjustment is triggered when $t_{\text{search}} \geq T_{\max}$. If this condition is met, the satellite will transition from a search state to a reallocation state where it either (1) switches to a different target or (2) requests external assistance, such as a new tracking tip from another sensor or ground station.

**Incoming State Updates via Information Sharing** This process facilitates real-time adjustments to a satellite's tasking priorities based on state updates received from other satellites or ground stations. When a satellite receives a tracking tip message, $\mathcal{M}_{\text{track}} = (t_k, \mathbf{x}_k, \mathbf{P}_k)$, the satellite must update its internal state and tasking. This event is interpreted as an unprompted observation of the environment and the following process occurs

- *State and Covariance Update*: The satellite updates its own track catalog state estimate $\mathbf{x}_k$ and covariance $\mathbf{P}_k$ using the received tracking tip $\mathcal{M}_{\text{track}}$.
- *Recomputing the Uncertainty Search Volume*: After updating the state and covariance, the satellite recalculates the uncertainty search volume.
- *Regenerating Search Tasks*: With the updated search volume, the satellite regenerates its' candidate search tasks and scheduling promotion is reconsidered along side other satellite tasking.

**Observation Association Confusion** Addresses scenarios where multiple potential targets or clutter lead to ambiguous observations. When an observation $\mathbf{z}_k$ has a similar Mahalanobis distance to multiple tracks $\{\mathbf{z}_{k_1}, \mathbf{z}_{k_2}, \dots\}$ (e.g. $D(\mathbf{z}_k, \hat{\mathbf{z}}_{k_1}) \approx D(\mathbf{z}_k, \hat{\mathbf{z}}_{k_2}) \approx \dots$), it becomes challenging to associate the observation with a specific target. In such cases, the satellite's policy will trigger a disambiguation routine that involves increasing maximum track hypothesis threshold, and increasing the observation cadence to gather more data points rapidly.

**Task Priority Adjustment for Sub-Optimal Uncertainty Convergence** Handles situations where the uncertainty in the estimated state of a target does not decrease as expected, despite continuous observations. Let $\sigma_k^2$ denote the total state uncertainty at time $t_k$, and assume the desired uncertainty at the end of a planning horizon is $\sigma_f^2 \to c$ as $k$ increases, where $c$ is the desired maximum uncertainty. If the observed convergence rate $d\Delta\sigma_k^2/dt$ is above a predefined threshold after the planning horizon, the satellite will:

$$\text{If } \Delta\sigma_k^2 \geq \varepsilon_{threshold}, \text{ increase priority of alternative tasking actions} \tag{16}$$

Actions may include altering the observation strategy (e.g., changing the sensor's pointing direction or integration time), initiating cooperative observations with other satellites, or adjusting the processing parameters in the state estimation algorithm.

### 4.3 Performance Metrics

**Time to Search Uncertainty Region** The time required to complete the search region is an important metric for evaluating the efficiency of localized search actions. This metric is defined as the cumulative time required for a sensor to perform all scheduled search tasks until the target is detected within the sensor's field of view. Mathematically, this can be expressed as:

$$t_{\text{search}} = \sum_{k=1}^{n_{\text{tasks}}} t_{\text{task},k} \quad \text{subject to} \quad \mathbf{p}_{\text{c},k} \cdot \mathbf{r}_{\text{t}} \leq \frac{\theta_{FOV}}{2},$$

where $t_{\text{task},k}$ represents the time needed to execute each search task $k$, and the constraint ensures that the target is detected within the field of view (FOV) of the sensor, defined by the pointing configuration $\mathbf{p}_{\text{c},k}$ and the FOV half-angle $\frac{\theta_{FOV}}{2}$.

**Expected Track Accuracy** The expected track accuracy is evaluated based on the total variance $\sigma^2$ of the estimated state over time. For a given target state $\mathbf{x}_k$ with associated covariance matrix $P_k$, the total variance can be quantified as:

$$\sigma^2(t) = \text{Tr}(P_k),$$

where $\text{Tr}(P_k)$ is the sum of the diagonal elements of $P_k$, representing the uncertainty in all state components. Lower values of $\sigma^2(t)$ indicate higher accuracy in tracking the target's position and velocity. This metric is particularly relevant when evaluating the effectiveness of the observation schedule, as the goal is to minimize $\sigma^2(t)$ and maintain an accurate track of the target.

## 5. RESULTS

The tools developed were used to simulate a localized target search mission in an edge case where a non-cooperative target is detected executing a maneuver from LEO into a earth-moon transit. We've assumed a worst-case scenario in which an external sensor was able to collect minimal observations of the target and reconstruct state vectors with relatively large uncertainty. This target state and uncertainty is used as the initial tipping message to generate localized search tasking or tracking tasking on a sensor-by-sensor basis. The scope of this work did not include the development or implementation of cislunar IOD aglorithms; thus, the additional assumption was made that the target's track was initialized with a 100 km position error sigma and 0.1m/s velocity error sigma.

The simulation included six space-based sensors with distinct orbits and measurement capabilities. Table 1 provides an overview of the sensor characteristics, including their FOV, measurement models, and the number of scheduled observations for each sensor.

Table 1: Summary of sensor configurations used in the simulation, including their orbital parameters, field-of-view (FOV) dimensions, measurement models, and the number of scheduled observations during the target's Earth-Moon transit.

| Sensor Orbit | Field of View | Measurement Model | # of Scheduled Observations |
|---|---|---|---|
| L2 Halo | $1.25 \times 1.25$ | $(\alpha, \varepsilon, \dot{\alpha}, \dot{\varepsilon})$ | 0 |
| L1 Halo | $0.25 \times 0.25$ | $(\alpha, \varepsilon, \dot{\alpha}, \dot{\varepsilon})$ | 10 |
| Butterfly | $3 \times 3$ | $(\alpha, \varepsilon)$ | 0 |
| Distant Retrograde | $1 \times 1$ | $(\alpha, \varepsilon)$ | 115 |
| 3:1 RPO | $4 \times 4$ | $(\alpha, \varepsilon, \dot{\alpha}, \dot{\varepsilon})$ | 20 |
| 4:1 RPO | $1 \times 1$ | $(\alpha, \varepsilon, \dot{\alpha}, \dot{\varepsilon})$ | 0 |

Figure 4 shows the generation of uncertainty-based search regions projected onto the sensor's reference frame. Sensors were tasked to perform raster scans over these regions, effectively reducing the uncertainty in the target's position and improving the likelihood of reacquisition after periods of limited sensor availability. At each critical decision points, a search task was selected, and scheduled. Upon target detection, the target was tracked with limited observations.

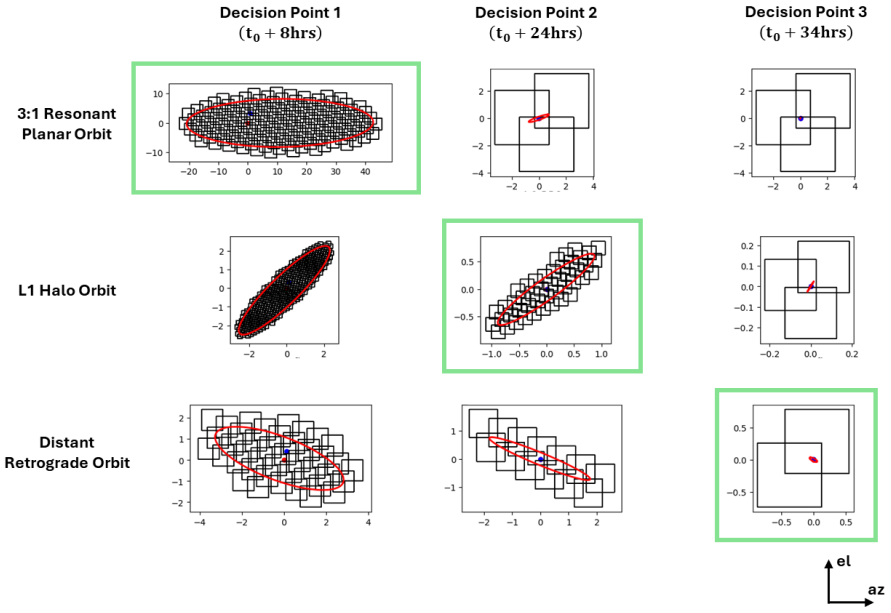


Fig. 4: Each decision point represents the selected time and search task that was chosen to be scheduled. Search regions with the green outline indicate the selected search task and the remaining candidate search are shown to contrast the selected tasks against the rejected tasks.

An Extended Kalman Filter (EKF) was used for dynamic state estimation, processing the generated observations to continuously update the target's estimated state and manage uncertainty.

Synthetic observations were generated by each sensor at specific time windows during the target's Earth-Moon transit. These observations were spaced to reflect availability and operational constraints of space-based sensors in cislunar space. Throughout the transit, the target spacecraft's state was successfully estimated and updated, with the EKF managing the uncertainty effectively. The use of collaborative tracking and information sharing between sensors significantly enhanced overall tracking accuracy. Figure 5 shows the estimated track accuracy throughout the planning horizon.

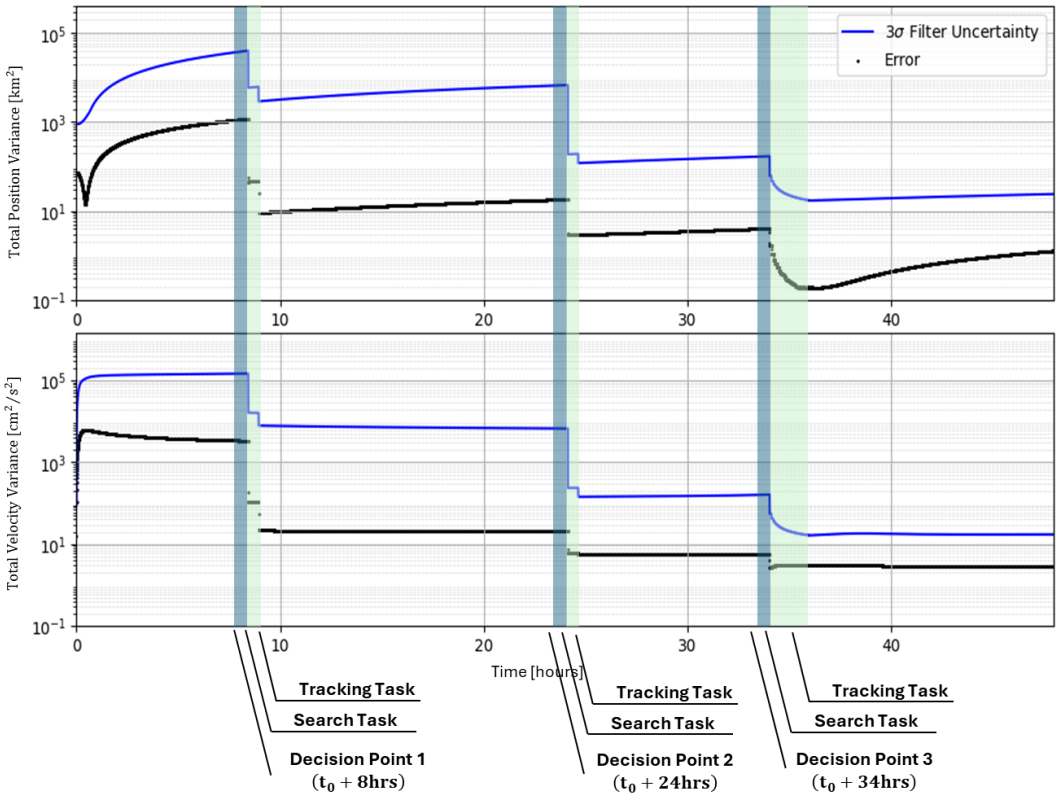


Fig. 5: Shows the state estimation performance for the various sensors tasked to search for and track the object in transit between the Earth and Moon. For the selected scenario, the sensor in a 3:1 resonant planar orbit observed the target object 20 times after the first decision point, the sensor in a L1 Halo orbit observed the target object 10 times after the second decision point, and the sensor in a distant retrograde orbit observed the target object 115 times after the third decision point. A total of 145 observations were scheduled throughout the 48 hour planning horizon.

## 6. CONCLUSION

The proposed tracking and sensor scheduling framework for cislunar space demonstrated robust performance in managing uncertainty, optimizing sensor resources, and maintaining accurate tracking of non-cooperative targets. By leveraging localized search regions, collaborative tracking, and a semi-Markov Decision Process (sMDP) for sensor scheduling, the framework effectively addressed the challenges inherent in tracking objects in the Earth-Moon system. The results indicate that this approach can be a valuable tool for space situational awareness in the increasingly complex cislunar environment.

Future work could explore the integration of more sophisticated search strategies that account for probabilistic distributions within the uncertainty region, potentially improving search efficiency and reducing the time to reacquire targets. Additionally, a more comprehensive analysis can be performed by incorporating an IOD solution for cislunar objects [4]. These enhancements would further strengthen the ability of space-based systems to maintain comprehensive situational awareness in cislunar space.

## 7. REFERENCES


[1] Eddy, D. and Kochenderfer, M. Markov Decision Processes for Multi-Objective Satellite Task Planning. *2020 IEEE Aerospace Conference, Big Sky, MT*, 2020.

[2] Woffinden, D.C. *Angles-Only Navigation for Autonomous Orbital Rendezvous*. PhD thesis, Utah State University, 2008.

[3] Vallerie, E.M. Investigation of Photometric Data Received from an Artificial Earth Satellite. Master's thesis, Airforce Institute of Technology, 1963.

[4] Hofer, G.P., Jones, G.G., and Oldroyd, W.J. Post-Maneuver UCT Correlation Using Multi-Source Data Streams. *Advanced Maui Optical and Space Surveillance Technologies Conference (AMOS)*, 2024.

[5] Carpenter, J.R. and D'Souza, C.N. Navigation Filter Best Practices. Technical report, NASA Engineering and Safety Center, Hampton, Virginia, 2018.

[6] Holzinger, M.J. A Primer on Cislunar Space. *Airforce Research Laboratory*, 2021.